

Data-driven Dynamic-classifiers-based Seismic Failure Mode Detection of Deep Steel W-shape Columns

Mohammad Sadegh Barkhordari¹, Mohsen Tehranizadeh^{1*}

¹ Department of Civil & Environmental Engineering, Amirkabir University of Technology (Tehran Polytechnic), Tehran 1591634311, Iran

* Corresponding author, e-mail: tehranizadeh@aut.ac.ir

Received: 30 October 2022, Accepted: 11 May 2023, Published online: 22 May 2023

Abstract

It is vital to assess the health of buildings following a major earthquake. New technologies such as deep learning algorithms have grown increasingly tempting in such rapid applications because of their increased reliabilities and simplicity to traditional methods. Due to the kinematics of steel moment frames, inelastic deformations tend to concentrate within the steel column during an earthquake, resulting in local or global buckling. Rapid failure mode detection of the existing deep steel W-shape columns (DSWCs) cannot be quickly identified due to a lack of comprehensive empirical and mechanics-based models. This research proposed a machine learning (ML) algorithm based on the state-of-the-art techniques of dynamic classifiers for failure mode forecasting of the DSWCs using an experimental database and illustrated why the ML model suggests a specific failure mode for a particular sample. The database was created by combining 939 instances from various studies that have been published. A total of six machine learning models based on Dynamic Selection strategy were implemented. Three metrics, i.e., accuracy, precision, and recall, were used to evaluate the performance of models. As a result of the extensive examination, a machine learning model based on the META-DES model was proposed. In the training stage, Overall Local Accuracy, A-Priori, and META-DES algorithms, received the highest score (>0.96) across all criteria. The META-DES model correctly predicted the failure mode of the DSWCs with an accuracy of 0.907 in the testing phase. The META-DES algorithm performed better than previous methods which are employed to identify the failure mode.

Keywords

steel W-shape column, machine learning, failure mode, dynamic classifiers, data-driven approach

1 Introduction

Steel moment-resisting frames are utilized in earthquake-prone areas around the world to keep plastic deformations in the beams while the columns remain elastic. Accordingly, some principles and methods are used. For instance, steel beams and columns are designed for lower seismic loads and a combination of the capacity design as well as increased seismic loads, respectively [1]. In some circumstances, these techniques will not be able to eradicate plastic hinges in first-story columns. For example, the first mode of frame buildings is assumed in strong-column-weak-beam design to establish the column strength requirement; however, this is frequently violated, notably in midrise to high-rise buildings [2]. In addition, first-story columns of steel frame buildings are prone to experiencing inelastic rotation demands due to the formation of a full-frame yield mechanism and force redistributions that occur as a component's strength and stiffness deteriorate [3, 4].

In the United States and elsewhere, deep steel W-shape columns (DSWC) are commonly utilized in special steel moment resisting frames to give ductile behavior during an earthquake [5]. For two reasons, the failure mode identification of columns is a source of worry. First, the plastic deformation weakens the column ends, making them vulnerable to local and global buckling [6, 7]. This is especially concerning because, unlike beams, columns cannot easily be braced to prevent buckling. Furthermore, because steel columns frequently transport significant axial force and are along the vertical load path, their degradation of axial load carrying capacity has serious consequences for global collapse [6, 7]. Scholars have investigated the behavior of the DSWCs experimentally or computationally. The use of extensive finite element analysis through parametric studies is a common method for discovering failure modes of DSWCs [8, 9]. Such a deep examination is valuable, but

it necessitates a significant amount of computing cost and effort, as well as time and resources to complete [4]. In practice, it is preferable to detect the failure mode as soon as possible following the occurrence of natural hazards in order to determine the damage evaluation or retrofiting options for the damaged structure. In such cases, the use of machine learning (ML) approaches offers a viable alternative to comprehensive numerical analysis.

In recent years, ML approaches have attracted a lot of attention by claiming to be applicable to all engineering fields. There is a rising interest in applying ML approaches to civil engineering procedures, particularly in the field of structural damage assessment. As an example, Mangalathu and Jeon [10] investigated several ML algorithms for estimating beam-column joint shear strength and also proposed probabilistic models to identify the type of failure mode of concrete beam-column joints. Several researchers investigated various ML models such as adaptive boosting, decision trees, random forests, and artificial neural network (ANN), to name but a few, for failure mode recognition of reinforced concrete (RC) columns [11–14]. Gao and Lin [15] applied eXtreme Gradient Boosting (XGBoost) to predict the RC beam-column joints' failure mode. Zhang et al. [16] implemented ML algorithms prediction of failure modes of RC shear walls. They reported that XGBoost and gradient boosting algorithms accurately predicted the failure modes of the RC shear walls. Chaabene and Nehdi [17] hybridized the atom search optimization (ASO) algorithm with ANN to develop a model for failure mode identification of steel fiber-reinforced concrete beams. Kabir et al. [18] proposed an algorithm based on the decision tree for identifying the failure mode of column base plate connections.

Since the DSWCs are one of the most important structural elements of steel buildings, and their post-seismic behavior is critical. However, no prior research has employed dynamic selection-based models to predict the failure mechanism of the DSWCs [19]. Moreover, the previous models' performance was poor [19]. This study aims to propose a model for accurately and reliably predicting the failure mode of the DSWCs using dynamic selection strategies. A database of 939 DSWCs subjected to axial-lateral loads was used to assess the applicability of ML models in detecting the failure modes of the DSWCs.

2 Experimental database

In this study, a database of DSWCs from the literature is used. The database contains a total of 939 DSWCs and is gathered by Sediek [19]. Input variables (Tables 1 and 2)

are considered including web slenderness ratio (h/t_w), flange slenderness ratio ($b_f/2t_f$), global slenderness ratio (L/r_y), torsional slenderness ratio ($J/(S \times h_0)$), axial load ratio (AxLoad), axial loading protocol (AxPro), boundary conditions (BouCon), and lateral loading protocol (LatPro). These variables are selected based on previous research (experimental and parametric studies) [9, 19]. The column's bottom is presumed to be completely fixed. Boundary conditions are recognized for the column top including (1) fully fixed in all planes (FF); (2) fixed in-plane rotation with free out-of-plane rotation (FP); (3) free in-plane rotation with a fixed out-of-plane rotation (PF); (4) in-plane rotation is restrained by a rotational spring or flexible beam element with fixed out-of-plane rotation (SF). There are five different forms of lateral loading protocols: symmetric cyclic (SC), monotonic (M), cyclic-monotonic (CM), cyclic ratcheting (CR), and asymmetric cyclic (AC). Axial loading procedures are divided into three categories: constant (C), symmetric cyclic (SC), and monotonic (M). In Table 1, h is web depth, b_f is the flange width, t_w is thickness, L is the total length, J presents the torsional constant, S presents the elastic modulus of the section (about the x-axis), h_0 presents the distance between flanges, and STD is the standard deviation of a random variable. Three types of failure modes are considered for DSWCs (Fig. 1): (1) local buckling near its ends, which is referred to as local failure (LF); (2) global failure (GF), a DSWC that fails in a global flexural or lateral-torsional mode without considerable local buckling; (3) the DSWC has significant local buckling as well as a global flexural or lateral-torsional failure (GLF), regardless of which occurs first. The failure modes gathered from past studies are matched to these three types based on the available information in each study.

Table 1 Range of the input variables

Input variable	$b_f/2t_f$	h/t_w	L/r_y	$J/(S \times h_0)$	AxLoad
Std	1.51	11.73	20.90	0.00342	0.12154
Min	2.43	5.21	7.1	0.0004	0.0
Mean	5.44	34.61	71.24	0.00246	0.32435
Max	9.92	57.5	161.19	0.0383	0.75

Table 2 Distribution of the loading protocol and boundary conditions

Lateral loading protocol	SC	CR	AC	M	CM
Count	404	313	114	68	40
Boundary conditions	FF	BF	FP	PF	
Count	349	349	161	80	
Axial loading protocol	C	M	SC		
Count	694	225	20		

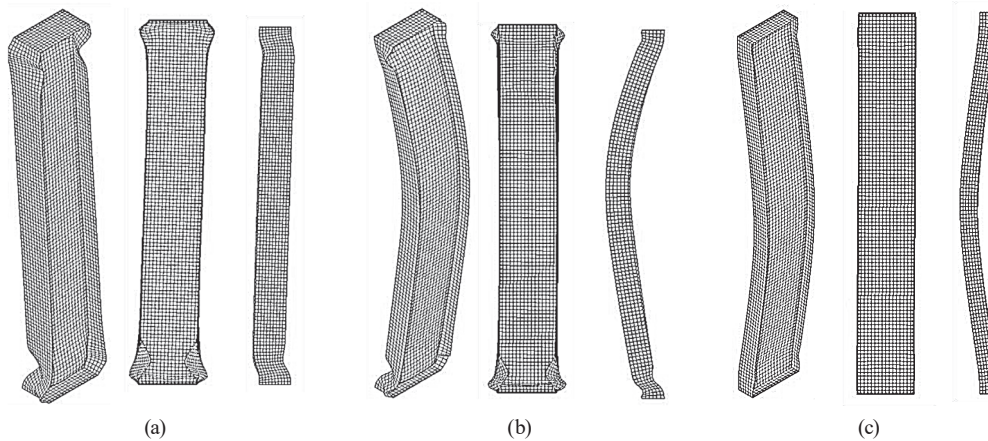


Fig. 1 Failure modes of DSW columns; (a) local failure (LF), (b) local buckling as well as a global flexural/lateral-torsional failure (GFL) and (c) global failure (GF)

3 ML models

Dynamic Selection (DS) refers to strategies in which the basic classifiers are chosen just-in-time for each new instance to be classed when making a prediction [20]. To forecast the label of a certain test sample, only the most skilled basic classifiers, or an ensemble including the most competent classifiers, are chosen. The justification for such systems is that each basic classifier is an expert in a particular limited area of the feature space, rather than every classifier being an expert in categorizing all unknown data. As a result, DS can often outperform any single model. This is in contrast to static selections, which involve selecting members only once, such as averaging outcomes from all basic classifiers in the model. DS offers two selection procedures, depending on whether a single classifier (known as Dynamic Classifier Selection (DCS)) or an ensemble (known as Dynamic Ensemble Selection (DES)) is employed. Both DCS and DES algorithms use Random Forest (RF) classifier as the basic classifier. RF is a method for supervised learning. It has the ability to be utilized for both categorization and regression. It's also the most adaptable and user-friendly algorithm. RF generates decision trees from randomly selected samples, and each tree yields a forecast. Finally, the algorithm uses voting to determine the best option. In this study, the number of trees in the forest and the maximum depth of the tree are 150 and 15, which are determined using Bayesian global optimization [21].

3.1 DCS-A-Priori and DCS-A-Posteriori

A-Priori and A-Posteriori are two algorithms for DCS. Consider a set of N classifiers $C_{j=1,\dots,N}$, each of which has been trained to address the M -class classification problem. For an unknown instance x^* , let us take into account the nearest neighbor ($R(x^*)$ or θ_j) of the space surrounding x^* .

$R(x^*)$ is characterized as the k -nearest neighbors in the training data set. The sample is allocated to this class if all classifiers ($C_{j=1,\dots,N}$) assign it to the same class. Otherwise, local accuracy ($LA_{j,k}(x^*)$) is computed. DCS-A-Priori defines $LA_{j,k}(x^*)$ as the percentage of the correctly classified sample in the local region $R(x^*)$. This algorithm has been named "A-Priori" since the class allotted by the classifier $C_{j=1,\dots,N}$ to test the sample x^* is not taken into account. In the "A-Posteriori" algorithm, the knowledge of the class allocated by the classifier $C_{j=1,\dots,N}$ to the test instance x^* is exploited. If the classifier C_j assigns the sample x^* to the class g_1 , in this case, $LA_{j,k}(x^*)$ is calculated as [22]:

$$LA_{j,k}(x^*) = \frac{N_{CP}}{\sum_{i=1}^M N_{iP}}, \quad (1)$$

where N_{CP} is the number of neighborhood samples of x^* that are correctly assigned by C_j to class g_1 and $\sum_{i=1}^M N_{iP}$ is the total number of neighborhood samples that are assigned by C_j to class g_1 . In other words, in the "A-Posteriori" algorithm, local accuracy is computed after each classifier C_j generates the output on the test instance x^* . It should be noted that both methods also weight each neighbor of x^* according to its Euclidean distance.

3.2 Overall Local Accuracy (OLA) and Local Classifier Accuracy (LCA)

In DCS-OLA, the competence level ($\delta_{i,j}$) of a classifier C_j is calculated as its categorization accuracy in the area of competence (θ_j) (Eq. (2)). To forecast the identity of the test sample, the classifier with the largest competence level is chosen.

$$\delta_{i,j} = \frac{1}{K} \sum_{k=1}^K P(w_l | x_k \in w_l, c_i), \quad (2)$$

where $P(w_i|x^* \in w_i, c_i)$ and w_i are posterior probability and the class predicted by the classifier C_j for the sample x^* , respectively. x_k is one instance in the area of competence θ_j and K is the number of neighbors. The DCS-LCA technique is identical to the DCS-OLA, with the exception that in the former, the local accuracy is evaluated for the entire region of competence in terms of output class (Eq. (3)).

$$\delta_{i,j} = \frac{\sum_{x_k \in w_i} P(w_i | x_k, c_i)}{\sum_{k=1}^K P(w_i | x_k, c_i)} \quad (3)$$

3.3 Meta-learning

In the meta-learning for the dynamic ensemble selection (META-DES) framework [23] in order to determine whether a base classifier (C_j) is capable enough to identify a given test sample, a meta-problem employs a variety of criteria pertaining to its behavior. The approach goes through a meta-training stage, which extracts meta-features from each sample in the training phase and dynamic selection datasets ($C_{j=1, \dots, N}$). The meta-features retrieved are then utilized to train the meta-classifier. The meta-classifier is trained to determine whether a base classifier C_j is capable of classifying a particular input sample. A Multinomial Naive Bayes (MNB) classifier usually is used as the meta-classifier. Meta-features for C_j in relation to the input are determined and supplied to the meta-classifier when an unknown instance is submitted to the algorithm. For the identification of the query example, the meta-classifier evaluates the competence level of the classifier C_j . Base classifiers with a skill level over a pre-determined criterion (competence level > 0.5) are chosen.

3.4 Dynamic Ensemble Selection performance (DES-P)

The area of competence θ_j is used to calculate the local performance of a base classifier in this method. The competence of the classifier C_j is then computed by the difference between the accuracy of the C_j and a random classifier (RC). The random classifier randomly selects a class with equal probabilities. The random classifier's performance is determined by the formula $RC = 1/NC$, where NC is the number of classes. As a result, the competence level $\delta_{i,j}$ in the DES-P method [24] is computed using Eq. (4).

$$\delta_{i,j} = \hat{P}(c_i | \theta_j) - \frac{1}{L}, \quad (4)$$

where $\hat{P}(c_i | \theta_j)$ is the accuracy of C_j in the area of competence θ_j , θ_j (or $R(x^*)$ in Section 3.1) is characterized as the

k -nearest neighbors in the training data set. The size of the region of competence (parameter k) is 5 for all models.

4 Results and discussion

In this study, accuracy (Eq. (5)), precision (Eq. (6)), and recall (Eq. (7)) are utilized as score indicators.

$$Accuracy = \frac{TP + TN}{TP + FP + FN + TN}, \quad (5)$$

$$Precision = \frac{TP}{TP + FP}, \quad (6)$$

$$Recall = \frac{TP}{TP + FN}, \quad (7)$$

where TP is the true positive, TN is the true negative, FP is the false positive, and FN is the false negative.

Six models, namely 'A-Priori', 'A-Posteriori', 'OLA', 'LCA', 'DES-P', and 'META-DES' are developed utilizing the python package DESlib to the failure modes of the DSWCs. The entire 939 data points are divided into two parts: 80% for the training phase and 20% for the testing phase. The prediction performance of the six ML models on the training set is shown in Fig. 2, considering all classes. As can be seen in Fig. 2, A-Priori, OLA, and META-DES models achieve the highest accuracy score. What stands out in Fig. 2 is the general pattern of the highest precision and recall scores of the A-Priori, OLA, and META-DES models. In contrast, the LCA and DES-P model presents the lowest accuracy, precision, and recall among the six ML models. It should be noted that precision and recall metrics are computed for each label, and their means are reported.

A confusion matrix (Fig. 3) is used to examine the performance of the different models on the testing data set. The confusion matrix is a square matrix of order n , where n is the number of categories (i.e., failure modes) analyzed in this paper; hence, n equals three. The confusion matrix's rows and columns correspond to the three true and forecasted classes. The number of successfully identified examples is shown by the diagonal members of the confusion matrix. The off-diagonal areas, on the other hand, represent the wrong cases, or the number of instances in a class that is misclassified. The overall accuracy, precision, and recall metrics are shown in the lowest cell on the right side, the column on the far right, and the row at the bottom of the confusion matrix, respectively. It is seen (Fig. 3(e)) that the META-DES model achieves the highest accuracy (90.78%) in the testing datasets. In Fig. 3(e), by observing the GLF mode, in which 2.8% is misclassified as the LF mode. Overall

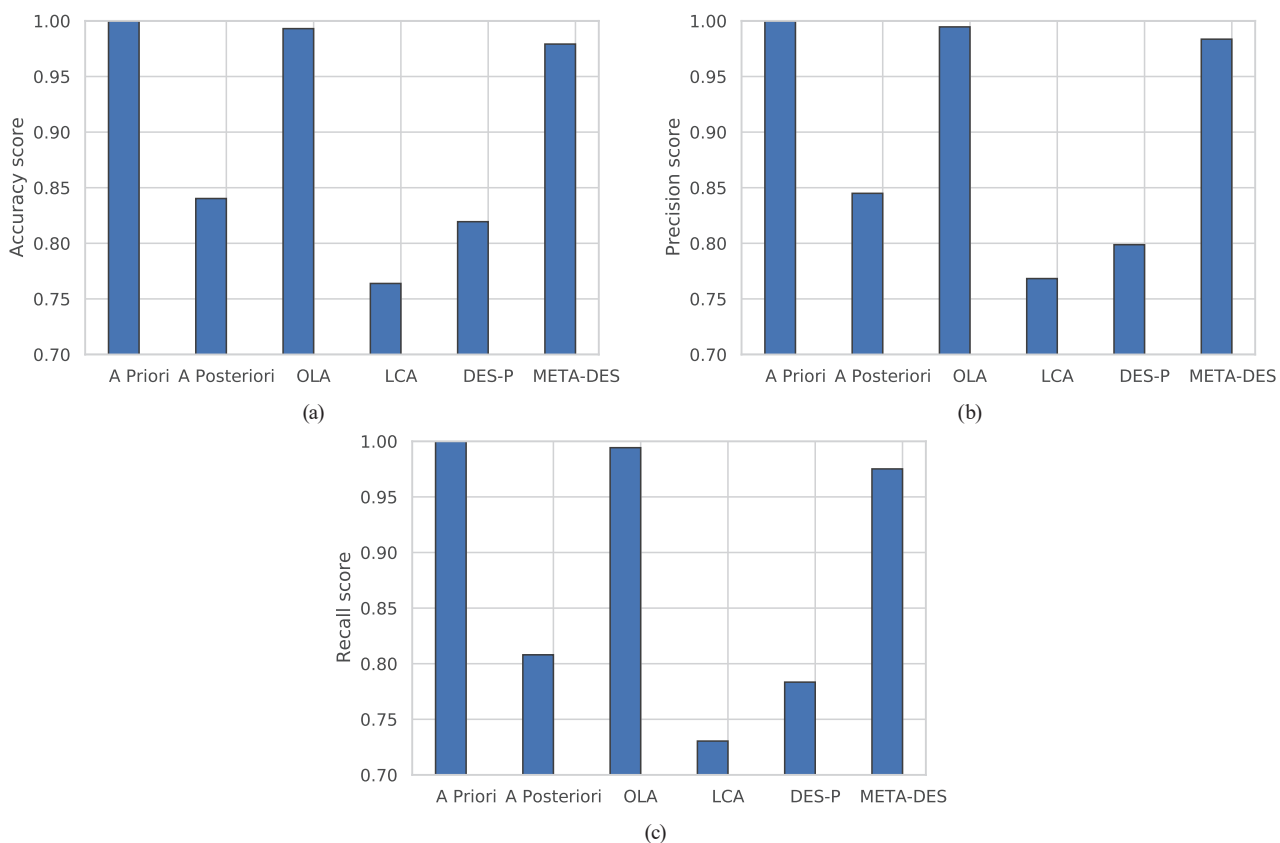


Fig. 2 Performance of different models - training dataset; (a) Accuracy score of models, (b) Precision score of models, (c) Recall score of models

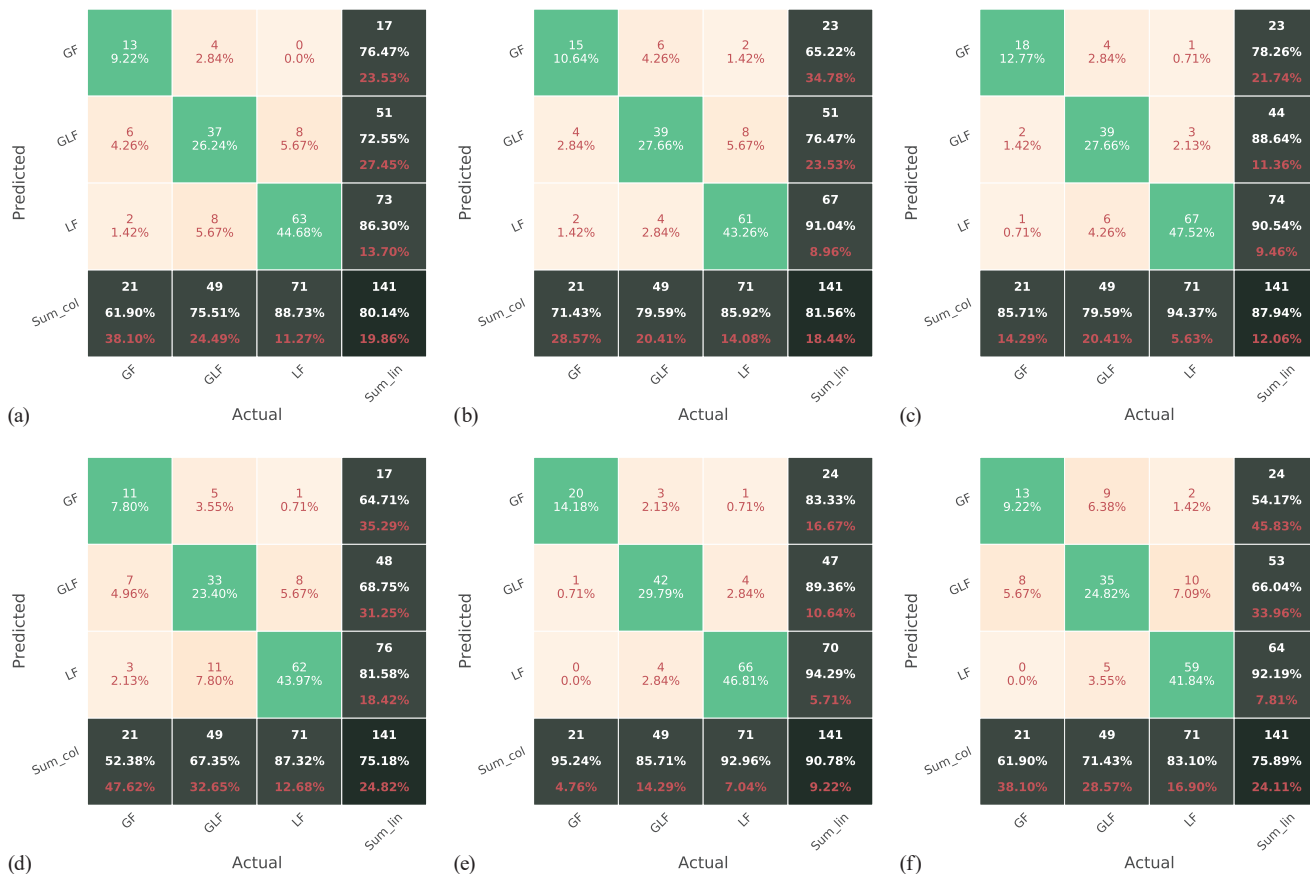


Fig. 3 Confusion matrix of the models; (a) A-Posteriori, (b) A-Priori, (c) DES-P, (d) LCA, (e) META-DES, (f) OLA

accuracies of the various models are A-Posteriori = 80.14%, A-Priori = 81.56%, DES-P = 87.94% LCA = 75.18% and OLA = 75.89%. What can be clearly seen is that recognizing the GLF mode is often challenging for most of the models since the OLA, LCA, A-Priori, and DES-P models have 54.17%, 64.71%, 65.22%, and 78.26% precision in identifying the GF mode in the testing phase, respectively. The largest amount of error in classification is related to the LCA model (Fig. 3(d)), in which 7.8% of samples with the GLF mode are misclassified as the LF mode. As can be seen from Fig. 3, the best performance (>85%) in terms of the precision score for the GLF mode is obtained using the META-DES and DES-P classifiers.

4.1 Partial dependence plot feature importance

Because standard ML models are "black box" models, it is also critical to decipher or explain the model prediction procedure. In this section, the impact of the input parameters on the failure mode prediction is investigated. As a result, the relative relevance of the META-DES model's input variable is derived using a partial dependence-based feature importance measure. As an example, the effect of $h/t_w - b_f/2t_f$ and $L/r_y - J/(S \times h_0)$ on each output (type of failure mode) is also shown in Fig. 4. Fig. 4(a) shows that the flange slenderness ratio of the section ($b_f/2t_f$) has a greater effect and as the value of $b_f/2t_f$ increases, their impact also increases and the model is more likely to predict the LF mode, which corresponds to a larger probability of flange buckling and yielding. Changes in the partial dependence (PD) values of the web slenderness ratio (h/t_w) are not notable signifying that h/t_w is less effective compared to $b_f/2t_f$. In other words, in the case of the LF mode, the web slenderness ratio has the most impact. Also, Fig. 4(a) shows the correlation value of two inputs (the figure placed on the right). The maximum correlation value is 0.61. The PD values obtained from the META-DES model for the global slenderness ratio (L/r_y) and the torsional slenderness ratio ($J/(S \times h_0)$) are plotted in Fig. 4(b). For L/r_y and $J/(S \times h_0)$, the PD value changes are about $(0.47-0.1) = 0.37$ and $(0.27-0.18) = 0.09$ for the GF mode class, respectively, which means that the feature L/r_y can influence predicting the GF mode more than $J/(S \times h_0)$ and high values of L/r_y increase the likelihood of the GF mode. The figure placed on the right show the maximum correlation value, which is 0.42. Moreover, the interaction between the target output and an input attribute of interest (e.g., linear, non-linear) is shown in Fig. 4. For instance, there is a definite non-linear link between $J/(S \times h_0)$ and the LF mode.

4.2 The influence of the region of competence

The purpose of this section is to investigate the effect of competence size on the performance of different models. The parameter (k) is varied from 3 to 15, and the performance of various techniques is evaluated using the test set. In Fig. 5, changes in accuracy vs. competence size are graphically presented. It is obvious that the parameter has an impact on the performance of some approaches. As an example, the accuracy score of the A-Priori model fluctuates between 0.78 and 0.88. Also, the accuracy of the A-Priori model reaches around 0.84 at the end, outnumbering the OLA, A-Posteriori, and LCA models. In addition, the LCA model, for almost all k values, performs the worst performance.

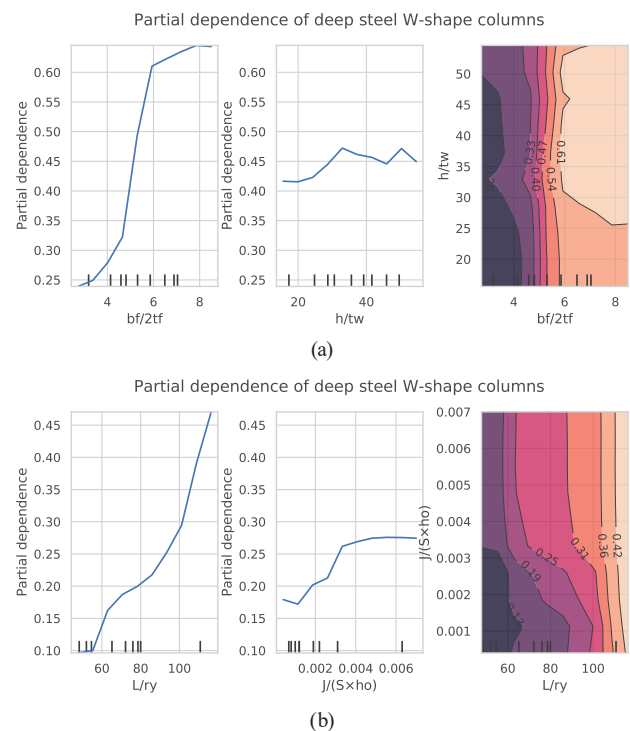


Fig. 4 Partial dependence graphs; a) LF mode, b) GF mode

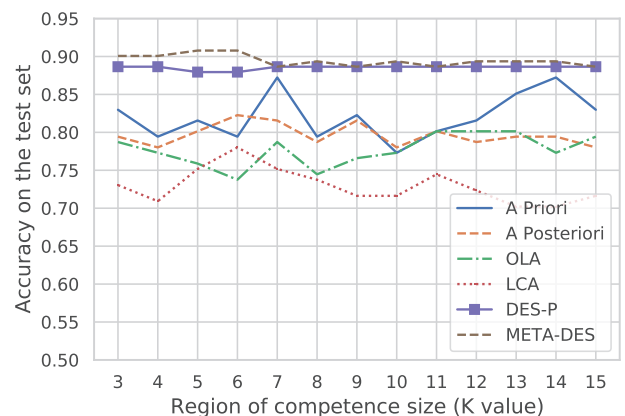


Fig. 5 Influence of the region of competence

Moreover, the performance of the DES-P and META-DES models doesn't change significantly when the competence size is changed.

5 Comparative study

In this section, the performance of the META-DES model is compared with ML algorithms that have previously been developed using the same database. Also, the effectiveness of the proposed classification criteria by Ozkula et al. [25] is contrasted with the effectiveness of the trained META-DES model. Sediek [19] utilized Linear discriminant analysis (LDA), naïve Bayes (NB), and K-nearest neighbor (KNN) algorithms to predict the failure mode of DSW columns DSWCs using the same database. Moreover, Ozkula et al. [25] suggested equations (Eqs. (8)–(9)) for determining the DSWCs' failure mechanism based on their geometric characteristics (i.e., web and flange dimensions).

$$\xi = \left(\frac{4ht_f}{C_s b_f t_w} \right) \left(\frac{t_f}{t_w} \right)^2, \quad (8)$$

$$C_s = \frac{2\pi c \cdot \sinh^2(\pi c)}{\sinh(\pi c) \cdot c \operatorname{inh}(\pi c) - \pi c}, \quad (9)$$

$$c = \frac{2 \frac{h}{b_f}}{3.93t\left(\frac{t_w}{t_f}\right) + 3.54}, \quad (10)$$

where ξ is the relative flexural stiffness ratio between the flange and the web, h is the web height, t_f is the flange thickness, t_w is the web thickness, and b_f is the flange width. The failure modes are determined based on the boundary values of ξ . A summary of the models' accuracy performance is shown in Table 3. The following is deduced from Table 3: 1) Two of the three ML methods (LDA and KNN,) have acceptable accuracy (i.e., more than 80%), 2) The accuracy of the KNN algorithm is slightly better than the LDA algorithm, which can be due to the fact that the KNN algorithm can consider inherent nonlinear decision boundaries to some extent [26], 3) Ozkula et al. [25]

method has the lowest accuracy value. This issue can be caused by the fact that in their method other crucial characteristics like the boundary conditions and loading protocols were not considered, and 4) The META-DES algorithm performs better than other models.

6 Conclusions

Deep steel W-shape columns (DSWC) can fail in local, global, or coupled modes, based on geometric features, boundary conditions, and so on. Producing new DSWCs or selecting suitable retrofit solutions for existing DSWCs necessitates determining the failure mode. This study used different dynamic-selection-based machine learning methods to identify the failure mode of the DSWCs, including 'A-Priori', 'A-Posteriori', 'OLA', 'LCA', 'DES-P', and 'META-DES'. The performance of various models is examined based on accuracy, precision, and recall metrics. The following conclusions can be drawn:

1. Among all the trained models, the META-DES model outperformed other models and obtained the highest accuracy (90.78%) in the testing phase.
2. The results showed that identification of the global flexural or lateral-torsional failure mode was often challenging for most of the models.
3. The partial dependence plot is used to analyze the influence of input variables on the failure mode prediction. The flange slenderness ratio of the section ($b_f/2t_f$) has a greater effect and as the value of $b_f/2t_f$ increases, their impact also increases, and the model is more likely to predict the LF mode.
4. The effect of the competence size on the performance of different models was evaluated. Changing the competence size did not have a significant effect on the performance of the DES-P and META-DES models.
5. The effectiveness of the trained META-DES model was evaluated against the effectiveness of previously developed ML models and classification criteria provided by other researchers. The results showed the META-DES model outperformed existing ML models and classification criteria.
6. When creating a model to determine the failure mode, crucial factors such the boundary conditions and loading protocols should be taken into account.

The META-DES model can also be employed as a general tool for determining DSWC failure modes. However, there is still room for improvement in this subject, such as

Table 3 Comparison of previous methods and the META-DES algorithm

ML method	Test accuracy (%)
LDA	83.7
NB	75.5
KNN	85.1
Ozkula et al. [25]	71.3
META-DES	90.78

using active learning to improve computation efficiency, developing a mechanics-guided failure mode detection framework based on machine learning for improved application, and so on.

Author Contributions: Conceptualization, M.S.B., M.T; methodology, M.S.B., M.T; software, M.S.B.; formal analysis, M.S.B.; writing – original draft preparation, M.S.B.; writing – review and editing, M.S.B.; supervision, M.T. All authors have read and agreed to the published version of the manuscript.

References

- [1] Barkhordari, M. S., Muntasir Billah, A. H. M. "Efficiency of Data-Driven Hybrid Algorithms for Steel-Column Base Connection Failure Mode Detection", *Practice Periodical on Structural Design and Construction*, 28(1), 04022061, 2023.
[https://doi.org/10.1061/\(ASCE\)SC.1943-5576.0000741](https://doi.org/10.1061/(ASCE)SC.1943-5576.0000741)
- [2] Elkady, A., Lignos, D. G. "Analytical investigation of the cyclic behavior and plastic hinge formation in deep wide-flange steel beam-columns", *Bulletin of Earthquake Engineering*, 13(4), pp. 1097–1118, 2015.
<https://doi.org/10.1007/s10518-014-9640-y>
- [3] Stoakes, C. D., Fahnestock, L. A. "Strong-axis stability of wide flange steel columns in the presence of weak-axis flexure", *Journal of Structural Engineering*, 142(5), 04016004, 2016.
[https://doi.org/10.1061/\(ASCE\)ST.1943-541X.0001448](https://doi.org/10.1061/(ASCE)ST.1943-541X.0001448)
- [4] Cravero, J., Elkady, A., Lignos, D. G. "Experimental evaluation and numerical modeling of wide-flange steel columns subjected to constant and variable axial load coupled with lateral drift demands", *Journal of Structural Engineering*, 146(3), 04019222, 2020.
[https://doi.org/10.1061/\(ASCE\)ST.1943-541X.0002499](https://doi.org/10.1061/(ASCE)ST.1943-541X.0002499)
- [5] Gutiérrez-Urzúa, F., Freddi, F., Di Sarno, L. "Comparative analysis of code-based approaches for seismic assessment of existing steel moment resisting frames", *Journal of Constructional Steel Research*, 181, 106589, 2021.
<https://doi.org/10.1016/j.jcsr.2021.106589>
- [6] Lignos, D. G., Hartloper, A. R. "Steel column stability and implications in the seismic assessment of steel structures according to Eurocode 8 Part 3", *Stahlbau*, 89(1), pp. 16–27, 2020.
<https://doi.org/10.1002/stab.201900108>
- [7] Islam, A., Imanpour, A. "Stability of wide-flange columns in steel moment-resisting frames: evaluation of the Canadian seismic design requirements", *Bulletin of Earthquake Engineering*, 20, pp. 1591–1617, 2022.
<https://doi.org/10.1007/s10518-021-01313-8>
- [8] Selvaraj, S., Madhavan, M. "Geometric imperfection measurements and validations on cold-formed steel channels using 3D non-contact laser scanner", *Journal of Structural Engineering*, 144(3), 04018010, 2018.
[https://doi.org/10.1061/\(ASCE\)ST.1943-541X.0001993](https://doi.org/10.1061/(ASCE)ST.1943-541X.0001993)
- [9] Sediek, O. A., Wu, T.-Y., Chang, T.-H., McCormick, J., El-Tawil, S. "Measurement, characterization, and modeling of initial geometric imperfections in wide-flange steel members subjected to combined axial and cyclic lateral loading", *Journal of Structural Engineering*, 147(9), 04021120, 2021.
[https://doi.org/10.1061/\(ASCE\)ST.1943-541X.0003086](https://doi.org/10.1061/(ASCE)ST.1943-541X.0003086)
- [10] Mangalathu, S., Jeon, J.-S. "Classification of failure mode and prediction of shear strength for reinforced concrete beam-column joints using machine learning techniques", *Engineering Structures*, 160, pp. 85–94, 2018.
<https://doi.org/10.1016/j.engstruct.2018.01.008>
- [11] Mangalathu, S., Jeon, J.-S. "Machine learning-based failure mode recognition of circular reinforced concrete bridge columns: Comparative study", *Journal of Structural Engineering*, 145(10), 04019104, 2019.
[https://doi.org/10.1061/\(ASCE\)ST.1943-541X.0002402](https://doi.org/10.1061/(ASCE)ST.1943-541X.0002402)
- [12] Feng, D.-C., Liu, Z.-T., Wang, X.-D., Jiang, Z.-M., Liang, S.-X. "Failure mode classification and bearing capacity prediction for reinforced concrete columns based on ensemble machine learning algorithm", *Advanced Engineering Informatics*, 45, 101126, 2020.
<https://doi.org/10.1016/j.aei.2020.101126>
- [13] Naderpour, H., Mirrashid, M., Parsa, P. "Failure mode prediction of reinforced concrete columns using machine learning methods", *Engineering Structures*, 248, 113263, 2021.
<https://doi.org/10.1016/j.engstruct.2021.113263>
- [14] Edward, C., Balu, A. S. "Failure Mode Recognition of Columns Using Artificial Neural Network", *IOP Conference Series: Materials Science and Engineering*, 936(1), 012044, 2020.
<https://doi.org/10.1088/1757-899x/936/1/012044>
- [15] Gao, X., Lin, C. "Prediction model of the failure mode of beam-column joints using machine learning methods", *Engineering Failure Analysis*, 120, 105072, 2021.
<https://doi.org/10.1016/j.engfailanal.2020.105072>
- [16] Zhang, H., Cheng, X., Li, Y., Du, X. "Prediction of failure modes, strength, and deformation capacity of RC shear walls through machine learning", *Journal of Building Engineering*, 50, 104145, 2022.
<https://doi.org/10.1016/j.jobbe.2022.104145>
- [17] Chaabene, W. B., Nehdi, M. L. "Novel soft computing hybrid model for predicting shear strength and failure mode of SFRC beams with superior accuracy", *Composites Part C: Open Access*, 3, 100070, 2020.
<https://doi.org/10.1016/j.jcomc.2020.100070>

Funding: This study receives no external funding for this research.

Institutional Review Board Statement: Not applicable.

Informed Consent Statement: Not applicable.

Data Availability Statement: Some or all data, models, or code that support the findings of this study are available from the corresponding author upon reasonable request.

Conflicts of Interest: The authors declare no conflict of interest.

- [18] Kabir, M. A. B., Hasan, A. S., Muntasir Billah, A. H. M. "Failure mode identification of column base plate connection using data-driven machine learning techniques", *Engineering Structures*, 240, 112389, 2021.
<https://doi.org/10.1016/j.engstruct.2021.112389>
- [19] Sediek, O. A. "Multiscale Simulation and Assessment of the Seismic Resilience of Communities, in *Civil Engineering and Scientific Computing*", PhD Thesis, University of Michigan, 2021.
<https://doi.org/10.7302/1337>
- [20] Cruz, R. M. O., Sabourin, R., Cavalcanti, G. D. C. "Dynamic classifier selection: Recent advances and perspectives", *Information Fusion*, 41, pp. 195-216, 2018.
<https://doi.org/10.1016/j.inffus.2017.09.010>
- [21] Nogueira, F. "Bayesian Optimization: Open source constrained global optimization tool for Python. 2014", [online] Available at: <https://github.com/fmfn/BayesianOptimization>
- [22] Didaci, L., Giacinto, G., Roli, F., Marcialis, G. L. "A study on the performances of dynamic classifier selection based on local accuracy estimation", *Pattern Recognition*, 38(11), pp. 2188-2191, 2005.
<https://doi.org/10.1016/j.patcog.2005.02.010>
- [23] Cruz, R. M. O., Sabourin, R., Cavalcanti, G. D. C., Ren, T. I. "META-DES: A dynamic ensemble selection framework using meta-learning", *Pattern Recognition*, 48(5), pp. 1925-1935, 2015.
<https://doi.org/10.1016/j.patcog.2014.12.003>
- [24] Woloszynski, T., Kurzynski, M., Podsiadlo, P., Stachowiak, G. W. "A measure of competence based on random classification for dynamic ensemble selection", *Information Fusion*, 13(3), pp. 207-213, 2012.
<https://doi.org/10.1016/j.inffus.2011.03.007>
- [25] Ozkula, G., Harris, J., Uang, C.-M. "Classifying cyclic buckling modes of steel wide-flange columns under cyclic loading", In: *Structures Congress 2017*, Denver, CO, USA, 2017, pp. 155-167. ISBN: 9780784480410
<https://doi.org/10.1061/9780784480410.014>
- [26] Barkhordari, M. S., Massone, L. M. "Failure Mode Detection of Reinforced Concrete Shear Walls Using Ensemble Deep Neural Networks", *International Journal of Concrete Structures and Materials*, 16(1), 33, 2022.
<https://doi.org/10.1186/s40069-022-00522-y>